International Journal of Engineering Trends and Technology
ISSN: 2231 – 5381 /doi:10.14445/22315381/IJETT-V70I3P229

Volume 70 Issue 3, 254-265, March 2022

Original Article

Concurrence of Process Optimized Parameters for Friction Stir Processed AA-6082-T6

Sukhvir Yadav[1], S. Sharma[2], B. Singh[3], P.B. Sharma[4]

[1]*Research Scholar Department of Mechanical Engineering, Amity University, Gurugram, India*
[2]*Associate Professor, Department of Mechanical Engineering, Amity University, Gurugram, India*
[3]*Assistant Professor, Department of Mechanical Engineering, J C Bose University of Science and Technology, Faridabad, India*
[4]*Vice-Chancellor, Amity University, Gurugram, India*

[1]sukhvirlisana@gmail.com, [2]ssharma26@ggn.amity.edu, [3]bhupee_28@yahoo.co.in

Abstract *- Being the structural component applications of Aluminum 6082-T6, the trend of experimentation in friction stir processing (FSP) has gained attention during the last decade and so. As FSP is a solid-state processing technique that provides conferred desired values of tensile strength, percentage elongation, the present motive of research is to obtain a set of optimized values for parameters of the process (like the tool rotation speed, traverse speed, and the number of passes). Twenty runs using three factors, three levels, which are chosen by CCD (central composite design) under randomized RSM (response surface method) reflected experimental results with the practical results. The optimized values of tensile strength and percentage elongation (responses) are 179 Mpa and 14.3% respectively also investigated values of input parameters such as tool rotation, traverse and the number of passes are 1284 rpm, 65mm/min, and 1 respectively.*

Keywords - *Friction stir processing, Response surface method, Tensile strength, Percentage elongation.*

I. INTRODUCTION

Wide range of engineering structural applications of AA 6082- T6 alloy demands stability in mechanical properties. The FSP has an upper edge for designees as compared to other conventional processing techniques for AA6082-T6 alloy. It is also an obvious choice of industries being a cleaner process with no harmful emissions but Devaraju et al. [1] evolved out the presence of manganese is mainly responsible for slagging in mechanical properties as being desired for the application-specific. Mehdi and Mishra [2] found a direct correlation of the mechanical properties with the selection of appropriate process parameters. The numerical models of responses for various levels of factors are designed by Ghanghas and Singhal [3] using the RSM technique. It is observed from literature reviews that there is a wide gap in the field of experimental correlation of FSPed AA6082-T6 alloy using the RSM technique. Makkar et al. [4] explored the modeling and process parameters optimization of FSWed AA 7039-T6 using RSM and GRA-PCA approach and concluded with greater tensile strength and yield strength by optimized parameters. Sharma and Sen [5] also tested FSPed optimized process parameters using two-way ANOVA, but lack in achieving the desired mechanical properties by varying all three input parameters. Meanwhile, Priyadarshani et al. [6] developed the effective RSM model for tensile strength of FSPed aluminum alloy and also succeeded to conclude correlation with input values. Moustafa et al. [7] experimented on Cu-Ni composites in FSP by varying the tool's rotation speed along with the traverse speed, groove width for getting the desired microhardness. Vignesh et al. [8] carried out the minimum possible number of experiments by the use of Taguchi orthogonal array (L_9) for aluminum nano surface composite and confirmed with experimental results. Kumar and Kumar [9] predicted the optimized values of the main process parameters values of FSPed specimens for maximizing the hardness and wear resistance of AA5083. Rathinasuriyan and Kumar [10] analyzed the multi-response process parameter optimization of dissimilar friction stir welding (FSW) aluminum alloy using gray relation analysis and found tool traverse speed as the significant parameter to get the desired result. Dinaharan et al. [11] optimized the FSW parameter using ANOVA with a 90.5% confidence level to achieve the desired value of hardness and percentage elongation of FSWed AA6061-T6. Maboud et al. [12] developed the artificial neural network to predict the tool wear rate relationship with the other process parameters involved during FSP. Rajakumar et al. [13] responded with RSM effectively to predict the responses of Al 1050 FSped specimens and concluded with the profound role of optimized values on mechanical properties. Mishra and Jain [14] developed the empirical relationship for the prediction of tensile strength of FSWed AA7075-T6. [1] predicted the performance of FSW characteristics by optimizing input parameters using the L_{16} Taguchi orthogonal array. Yadav.S et al. [15] investigated the mechanical properties of AA 6082 T6 alloy by altering the number of passes.

In the present experimentation, the CCD RSM approach was employed on AA 6082-T6 specimens by designing an L_{20} array with state ease software. The rotational speed of the tool, traverse speed of the tool, and the number of passes were found as inferential factors with

their three levels. The desired responses namely tensile strength and percentage elongation were analyzed with the same and their optimization goals lead to the optimized set of input parameters among numerous suggested solutions. An experimental relationship developed between input parameters and output responses. The optimal solution was determined. The conformity of the optimized solution was performed with post-analysis actual experimentation.

II. MATERIALS AND METHODS

The FSP input process parameters which are an influential effect on mechanical properties were chosen based on past research. Commercial AA 6082-T6 alloy was tested as the base material of dimension 220x30 mm (flat sample) of thickness 10mm was cut from the base plate. The chemical composition of AA6082-T6 as the base material is listed in table 1. The experimentation was performed on Vertical Milling Centre (VMC) (Sigma make) as shown in figure 1. The fixture arrangement had set up on the milling table has shown in figure 2. An octagonal pin-shaped tool made of D2 steel having pin length 6mm and shoulder diameter 25mm was used for experimentation as shown in figure 3. The edges on the tool help in material flow during stirring action.

The RSM is a mathematical tool utilized to optimize the independent variables that affect the response variables [16]. The experimental domain for RSM-CCD analysis is presented in table 2. Before the actual experimentation, the L_{20} array of the CCD RSM technique was considered for different parameters of the process and their respective levels. These twenty experiments provided their respective responses (namely TS and PE) which are tabulated in table 3. The specimens were prepared in dumb shape and had undergone tensile testing are shown in figure 4. Tensile testing was performed at room temperature UTM and tested specimens are shown in figure 5.

Table 1. Al-6082 T-6 Element-Wise Composition

Element	% Composition
Copper	0.00 – 0.10
Titanium	0.00 – 0.15
Zinc	0.00 – 0.25
Chromium	0.00 – 0.25
Iron	0.00 – 0.45
Manganese	0.35 – 1.05
Magnesium	0.45 – 1.15
Silicon	0.65-1.15
Aluminum	94.00 – 95.00

Fig. 1 Vertical milling machine

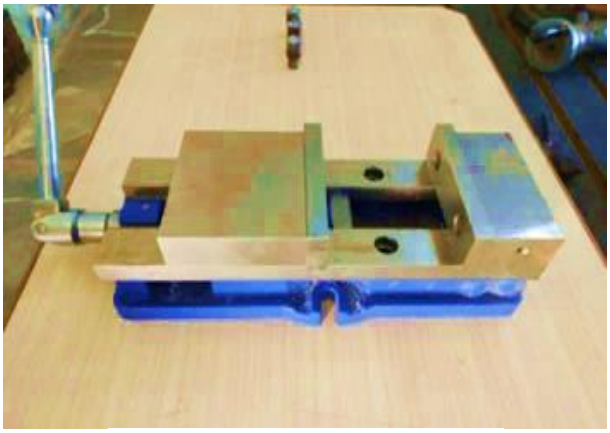

Fig. 2 Vertical milling table fixture

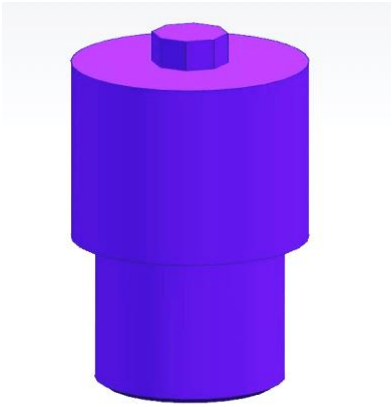

Fig. 3 D2 steel octagonal pin shape tool

Table 2. Experimental domain

Factor	Name	Units	Type	-1	0	+1
A	TRS	RPM	Numeric	1190	1480	1800
B	TTS	mm/min.	Numeric	43	65	84
C	NoP		Numeric	1	2	3

Table 3. Design experiment and their results

Run	A: Tool Rotation speed(rpm)	B: Traverse Speed(mm/min)	C: Number of Passes	Tensile Strength (Mpa)	Percentage Elongation
1	1480	65	3	165	18.5
2	1800	84	1	191	17
3	1190	65	2	180	14
4	1480	65	3	165	17
5	1190	43	3	165	18.5
6	1480	43	2	173	16.5
7	1800	43	3	161	19.5
8	1800	84	3	160	19
9	1480	65	2	166	16
10	1190	84	3	161	18.5
11	1800	43	1	191	10.5
12	1480	65	2	162	18
13	1480	84	2	165	15.5
14	1480	65	2	165	17.5
15	1480	65	2	166	16.2
16	1190	43	1	189	14
17	1480	65	2	164	15.5
18	1190	84	1	190	12.5
19	1480	65	2	174	16
20	1800	65	2	170	17

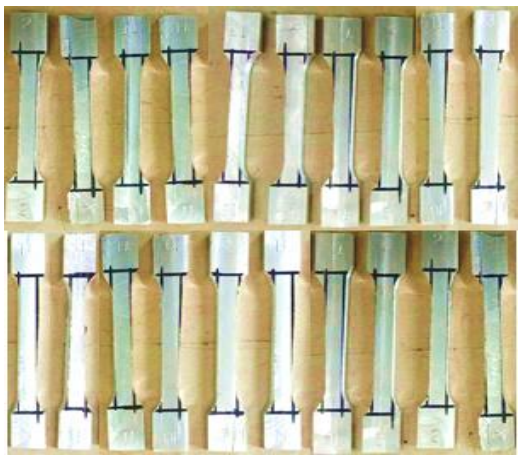

Fig. 4 Test specimen for tensile testing

Fig. 5 Test Specimen after Tensile Testing

III. RESULTS AND DISCUSSION

The investigation of input parameters' effect on response variables was conducted in the ambient environment. The specimens were cut longitudinally from the base plate. According to the hall patch relation, the tensile strength and grain size have an inverse relation [17]. The equation is $\sigma_y=\sigma_c+ k\ d^{(-1/2)}$, where σ_y is yield strength, σ_c material constant and d is grain size, The average TS (tensile strength) and percentage elongation was determined 171.15 Mpa and 16.36% respectively. Tensile testing graphs (load-extension) are shown in figure 6.

The observational relationship for response variables such as TS and PE (percentage elongation) was developed using the ANOVA technique. The model is quadratic and is significant for both responses (TS and PE) for calculating variables. The Fisher's F-test was conducted at a 95% confidence level for evaluating the developed model. For the model to be sufficiently adequate should have a higher F-value than the calculated. For the model to be significant lack of fit must be insignificant. The ANOVA for responses (tensile strength and percentage elongation) are depicted in table 4-5 The final equations in coded form for responses are given below

Tensile Strength = (168.26 - 1.20A - 1.20B - 13.48C + 0.2174AB - 1.04AC - 0.6935BC + 3.76A^2 - 2.41B^2 +7.17C^2) ***…… (i)***

% Elongation = (16.17 + 0.5359A + 0.3595B + 2.55C + 0.9633AB + 0.0692AC -0.6975BC - 0.1529A^2 + 0.4022B^2 – 0.3692C^2) ***…….……....(ii)***

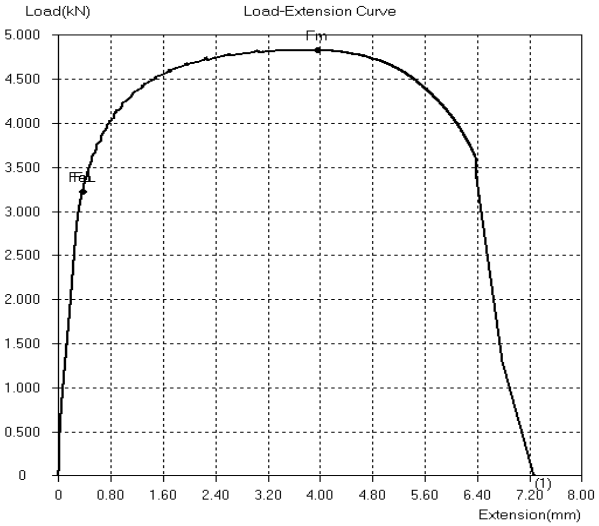

Fig. 6(a)

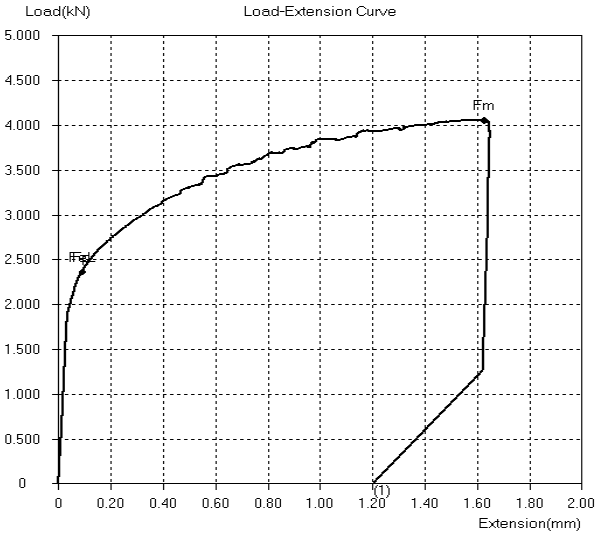

Fig. 6(b)

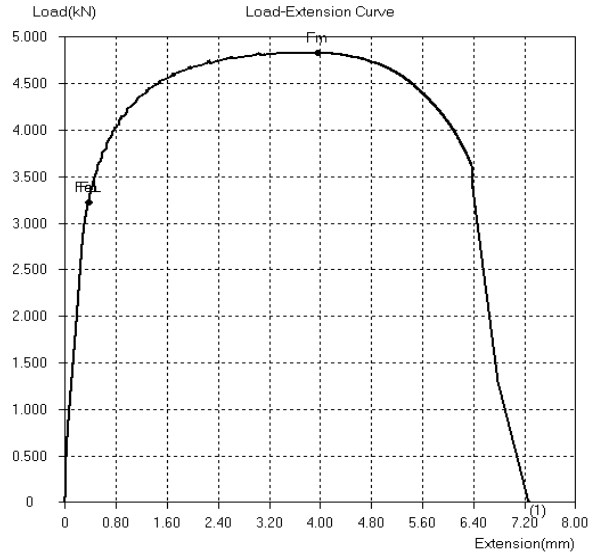

Fig. 6(c)

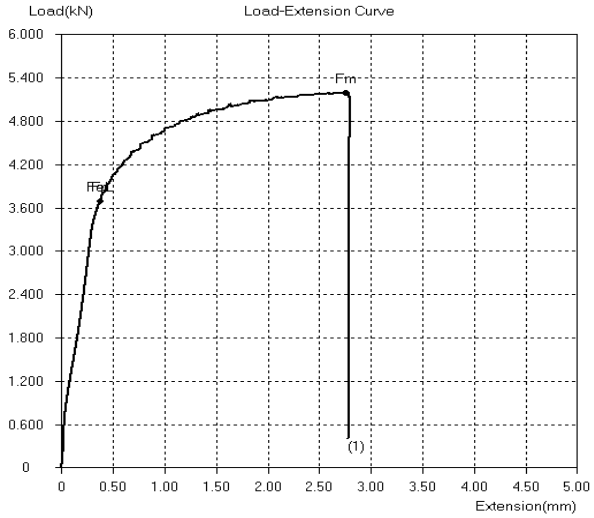

Fig. 6(d)

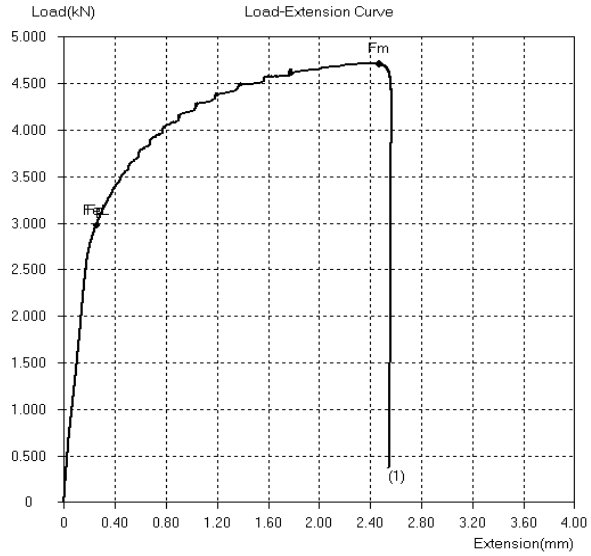

Fig. 6(e)

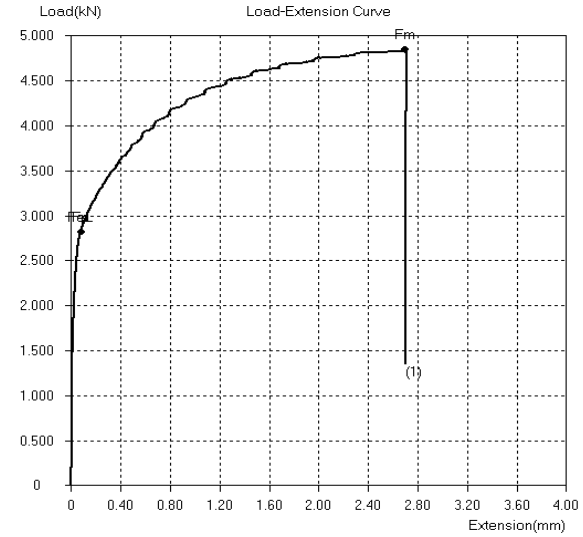

Fig. 6(f)

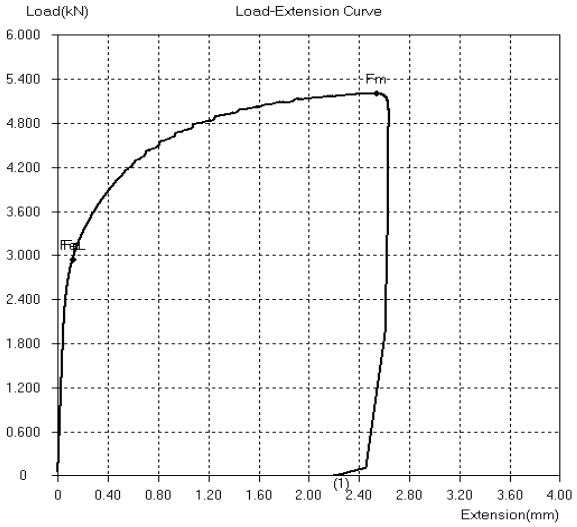

Fig. 6(g)

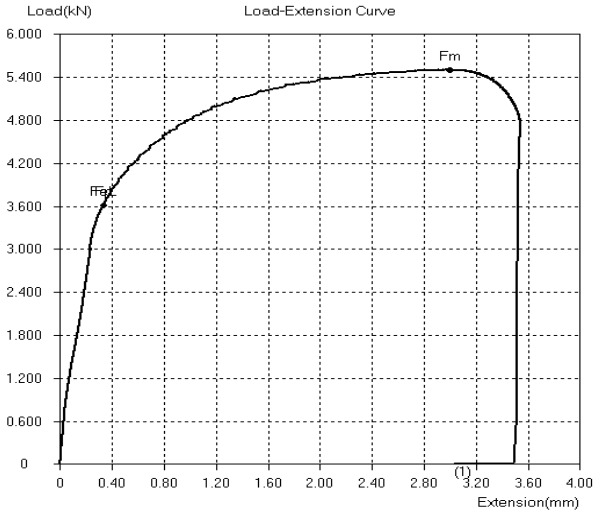

Fig. 6(j)

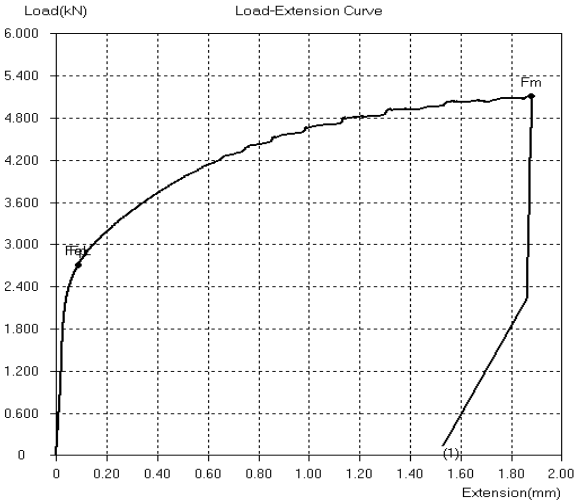

Fig. 6(h)

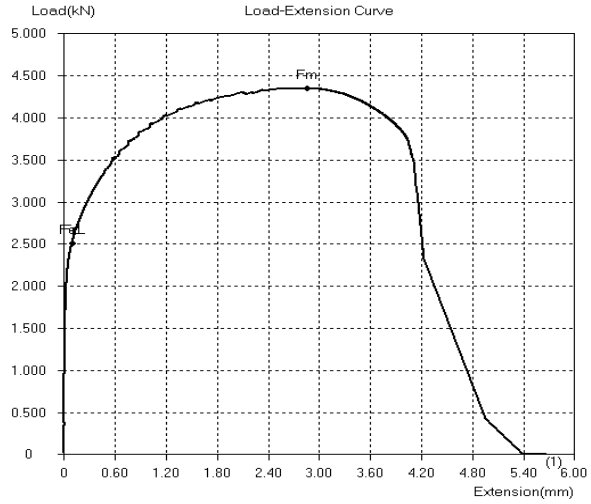

Fig. 6(k)

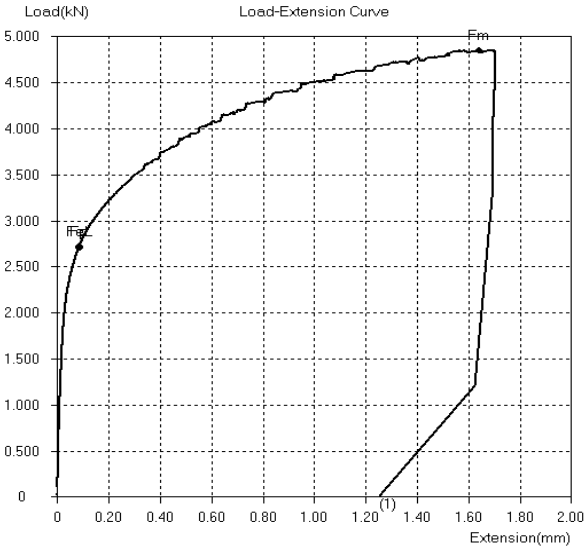

Fig. 6(i)

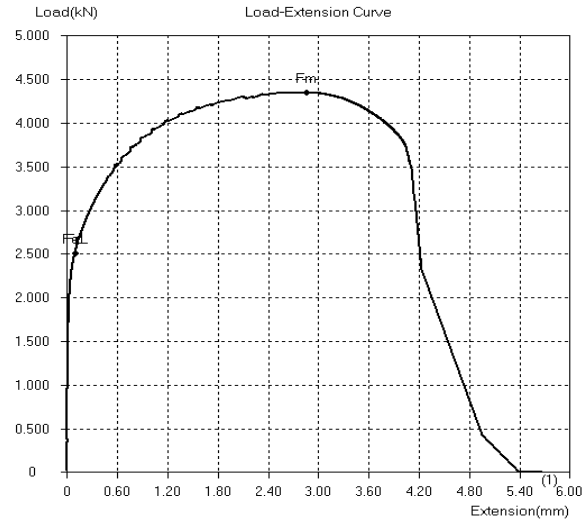

Fig. 6(k)

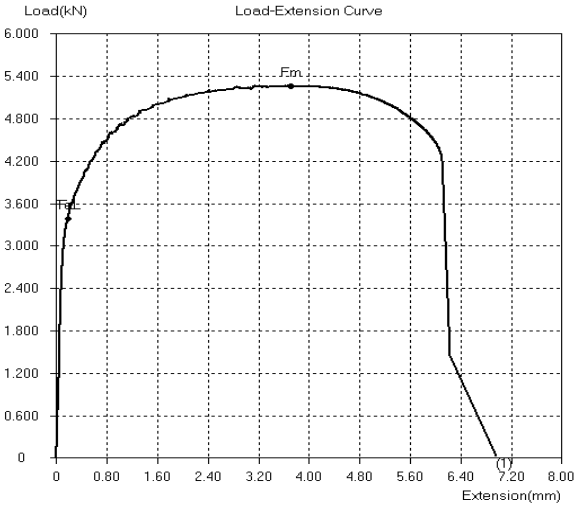

Fig. 6(l)

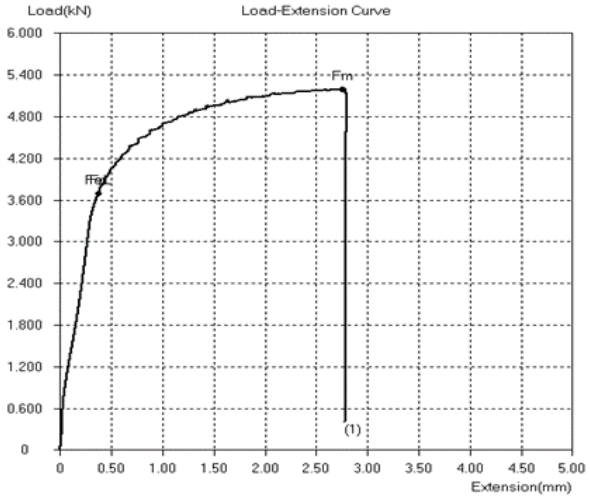

Fig. 6(o)

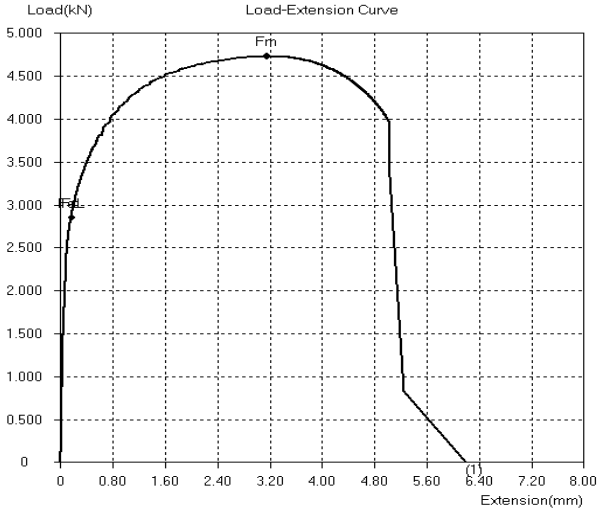

Fig. 6(m)

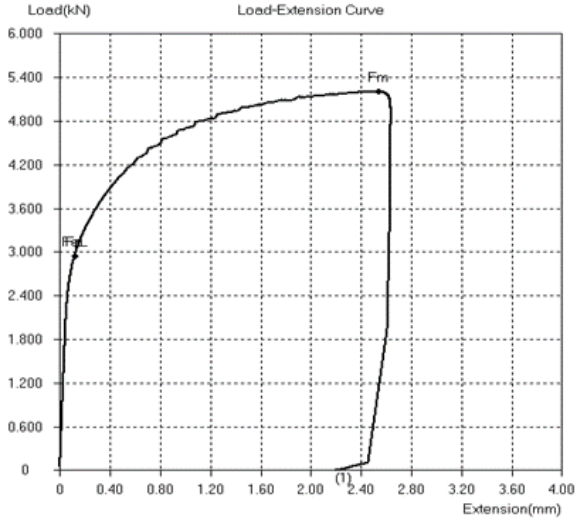

Fig. 6(p)

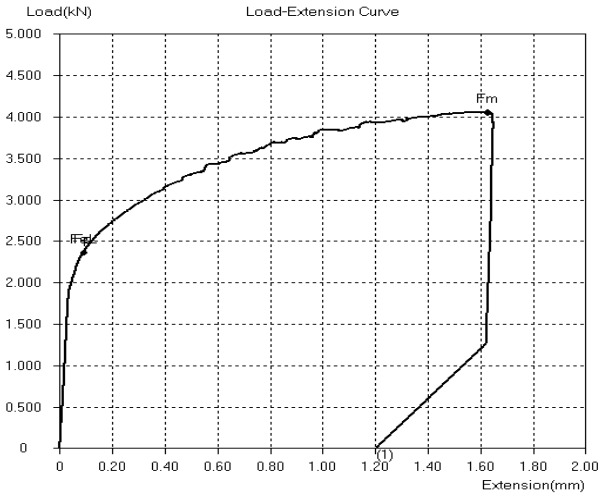

Fig. 6(n)

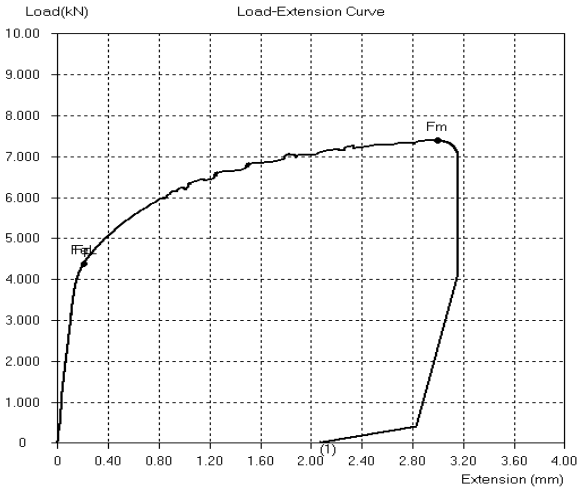

Fig. 6(q)

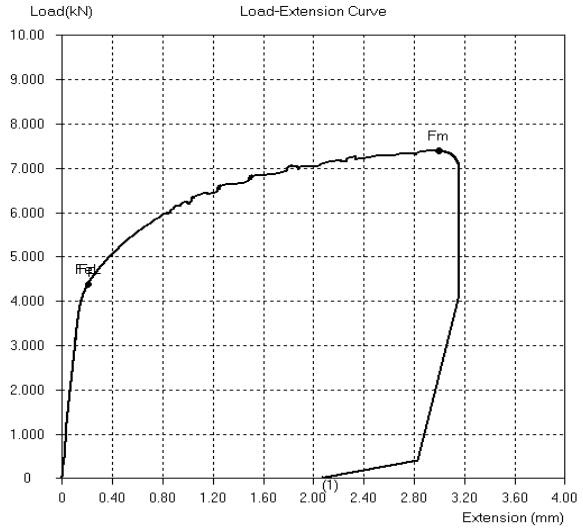

Fig. 6(r)

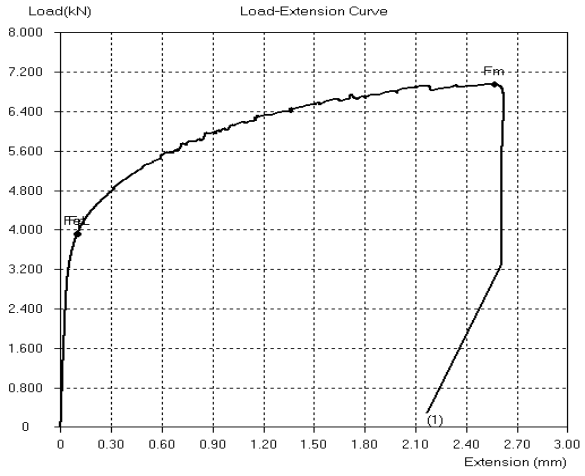

Fig. 6(s)

Fig. 6 Load-Displacement curves of specimen undergone tensile testing

ANOVA table for tensile strength w.r.t input variables has an F-value of 9.59 which means the quadratic model is highly significant. The acquired R-square values confirm the similarity between the experimental and anticipated results by the model, and (adj R^2) demonstrates the model's correctness. The absence of unimportant words is indicated by the proximity of R^2 and (adj R^2). A comparison of the range of predicted values at design points and average prediction errors is given by adequate precision (AP).

The signal-to-noise ratio is measured. The AP values suggest a good signal, and this model can be utilized to find the way through the design space. The standard error of the predicted value to the mean value of the actual response is represented by the coefficient of variance (CV).

The interaction between the input parameters AB, AC, and BC for TS; which is illustrated in Figure. 7, described the quadratic effect of factors on the response. Like-wise, the interaction between responses in case of % elongation under the combined effects of tool rotation speed, tool traverse speed, and the number of passes is depicted in Figure 8. The speculated vs actual values for TS and PE are shown in figure 9. The graph shows a close correlation between speculated and actual values. This means uncertainty is uniformly distributed throughout the model. It reveals the good adequacy of the developed regression model.

To maximize, the tensile strength and in range (10.5 to 19.5) percentage elongation, the numerical optimization suggested 100 solutions having the desirability equal to 1. The solution having the highest desirability 1 has 100% contribution of tensile strength and 100% contribution of percentage elongation as represented in the bar - graph in figure 10.

The FSP processing with suggested input parameters of solution 1 was confirmed with actual results which showed the proximity with optimized solution results. The point prediction at optimal responses is depicted in table 6. The comparison of suggested and actual results is tabulated in table 7.

Table 4. ANOVA for tensile strength

Tensile Strength						
Sources	**Sum of squares**	**df**	**Mean of square**	**F-Value**	**P-value**	
Model	2025.79	9	225.09	9.59	0.0008	significant
A-Tool Rotation Speed	14.47	1	14.47	0.6165	0.4506	
B-Tool Traverse Speed	14.35	1	14.35	0.6111	0.4525	
C-No. of Passes	1532.6	1	1532.6	65.28	< 0.0001	
AB	0.3785	1	0.3785	0.0161	0.9015	
AC	8.62	1	8.62	0.3672	0.5581	
BC	3.85	1	3.85	0.164	0.6941	
A^2	37.01	1	37.01	1.58	0.2378	
B^2	15.14	1	15.14	0.6449	0.4406	

C^2	124.72	1	124.72	5.31	0.0439	
Residual	234.76	10	23.48			
Lack of Fit	149.93	4	37.48	2.65	0.1376	not significant
Pure Error	84.83	6	14.14			
Cor Total	2260.55	19				
Std. Dev.	4.85		**R^2**	0.8961		
Mean	171.15		**Adjusted R^2**	0.8027		
C.V. %	2.83		**Predicted R^2**	0.4979		
			Adeq Precision	9.2698		

Table 5. ANOVA for Percentage elongation

Percentage Elongation						
Sources	**Sum of squares**	**df**	**Mean of square**	**F-Value**	**P-value**	
Model	76.42	9	8.49	3.94	0.0217	significant
A-Tool Rotation Speed	2.87	1	2.87	1.33	0.275	
B-Tool Traverse Speed	1.29	1	1.29	0.6002	0.4564	
C-No. of Passes	54.9	1	54.9	25.5	0.0005	
AB	7.44	1	7.44	3.45	0.0927	
AC	0.0383	1	0.0383	0.0178	0.8965	
BC	3.89	1	3.89	1.81	0.2084	
A^2	0.0613	1	0.0613	0.0285	0.8693	
B^2	0.4213	1	0.4213	0.1957	0.6676	
C^2	0.3309	1	0.3309	0.1537	0.7032	
Residual	21.53	10	2.15			
Lack of Fit	15.57	4	3.89	3.92	0.0672	not significant
Pure Error	5.96	6	0.9931			
Cor Total	97.95	19				
Std. Dev.	1.47		**R^2**	0.7802		
Mean	16.36		**Adjusted R^2**	0.5824		
C.V. %	8.97		**Predicted R^2**	-2.1951		
			Adeq Precision	7.6011		

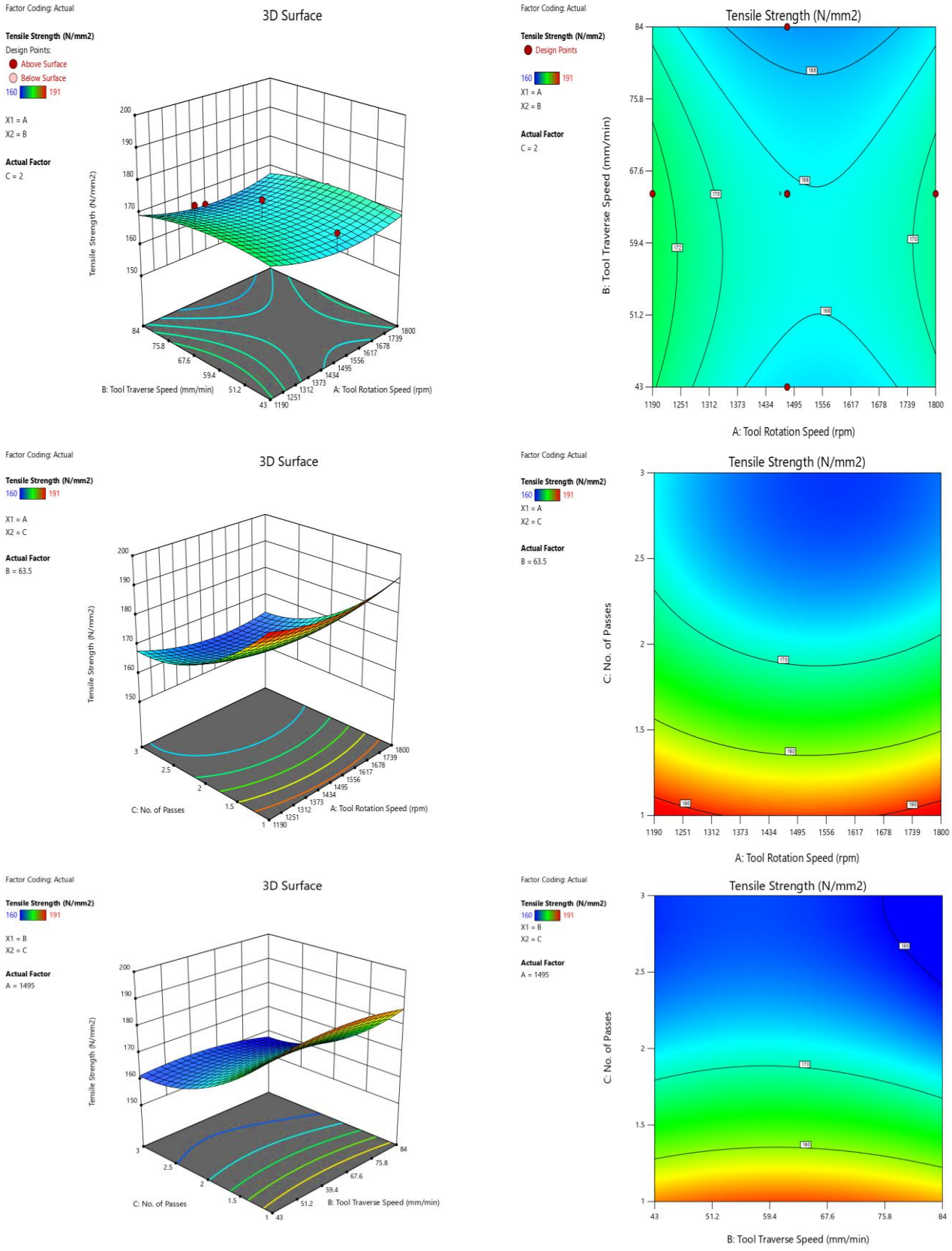

Fig.7 3D response surface plot and contour plot for tensile strength

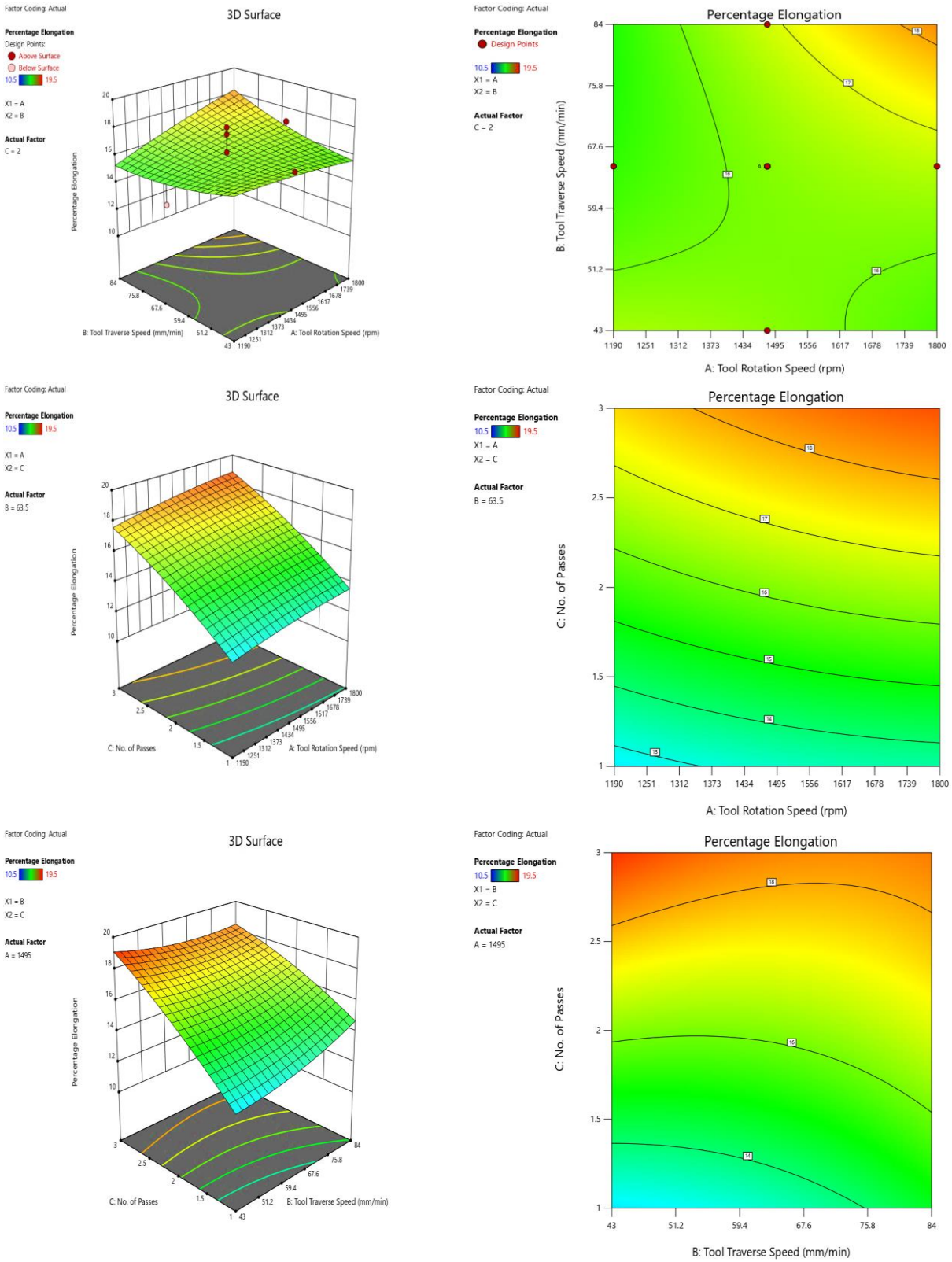

Fig. 8 3D response surface plot and contour plot for percentage elongation

Table 6. Point prediction at optimal responses

Response	Predicted Mean	Std Dev	SE Mean	95% CI Low for Mean	95% CI High for Mean	95% TI Low for 99% Population Mean	95% TI High for 99% Population Mean
Tensile Strength	168.257	4.8452	1.69451	164.481	172.033	145.304	191.211
Elongation	16.1708	1.4672	0.513123	15.0275	17.3141	9.2202	23.1215

Table 7. Response Confirmation after Experimentation of Optimized Solution

Factor A	Factor B	Factor C	Response - 1	Actual Value of Response - 1	%Age Deviation	Response - 2	Actual Value of Response - 2	%Age Deviation
1480	65	1	183.4	190.1	**3.52**	14.3	14.8	**3.37**

TRS (Factor – A in rpm), TTS (Factor – B in mm/min), NoP (Factor – C), TS (in N/mm2), Elongation (in %)

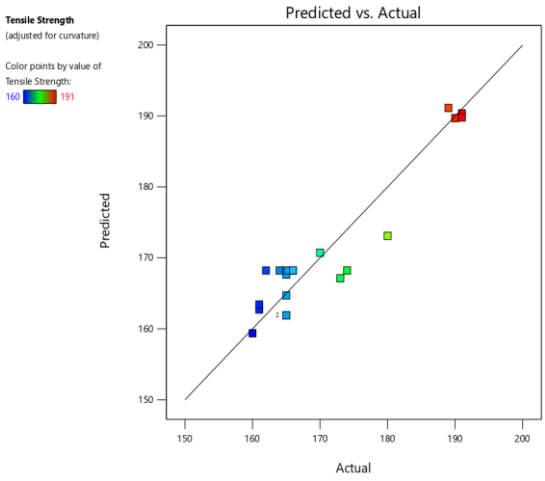

Fig. 9(a) Predicted vs Experimental Tensile strength

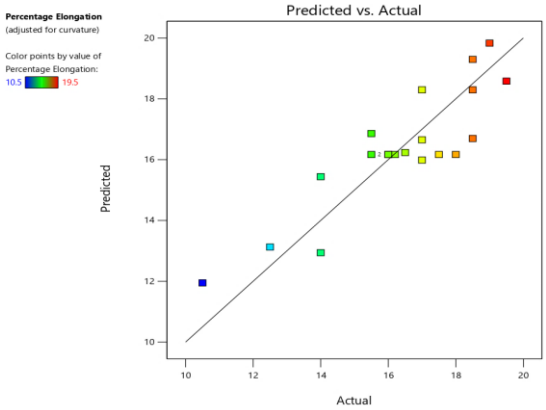

Fig. 9(b) Predicted vs Experimental %age elongation

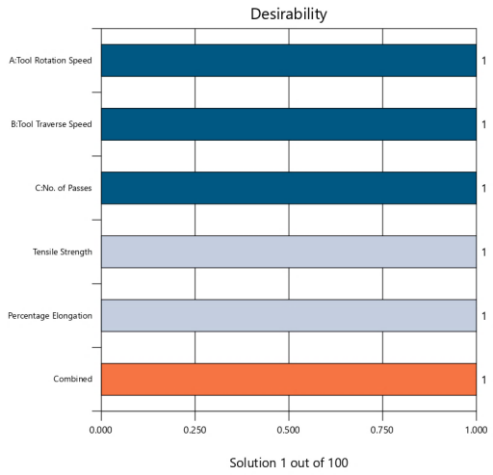

Fig. 10 Percentage contribution in cumulative desirability of each response & combined

IV. CONCLUSION

L_{20} RSM CCD array has proven its effectiveness to get the optimized values of input parameters and the same was confirmed with pre-and post-experimental trials. The effect of optimized factor values on desired response can summarize as under:

i. The number of experiments has been significantly reduced using the L_{20} RSM CCD model.
ii. The tensile strength of post optimized factors was found 3.6 % near the suggested value.
iii. The 100% desirability contribution of TS and PE in the combined optimization model was proven with only a 3.37% difference from actual values.

iv. The optimized value of TS and PE is 179 Mpa and 14.3% respectively whereas optimized values of input parameters are 1284rpm, 65mm/min, and 1 respectively.

The scope of the present work can be enlarged by increasing the levels of factors and also by increasing the number of responses to be optimized like surface roughness, microhardness, and yield strength.

ACKNOWLEDGMENT

The author would like to acknowledge M/s. Sunbeam Lightweighting Solutions Private Limited for their valuable support in material testing. The author would also like to thank M/s. Authentic Engineers Private Limited for providing base material in such a short period.

REFERENCES

[1] (2013). Devaraju A, Kumar A, Kumaraswamy A, et al., Influence of Reinforcements (Sic And Al2O3) and Rotational Speed on Wear and Mechanical Properties of Aluminum Alloy 6061-T6 Based Surface Hybrid Composites Produced Via Friction Stir Processing. Mater. Des. Elsevier Ltd;. [Online]. Available: www.dx.doi.org/10.1016/j.matdes.2013.04.029.

[2] (2020). Mehdi H, Mishra RS. Experimental Analysis and Optimization of Process Parameters of AA6061 and AA7075 Welded Joint By TIG+FSP Welding Using RSM. Adv Mater Process Technol. [Online]. Available: https://doi.org/10.1080/2374068X.2020.1829952.

[3] Ghangas G, Singhal S. Modelling and Optimization of Process Parameters for Friction Stir Welding of Armor Alloy Using RSM and GRA-PCA Approach. Mater Res Express. (2019) 6.

[4] Makkar G, Khurana S, Lata S. Optimization of Process Parameters in Friction Stir Processing Using Analysis of Variance (ANOVA). 15 (2018) 51–57.

[5] Sen U, Sharma K. Effects of Process Parameters of Friction Stir Processing on Tensile Strength of AA6063 Aluminum Alloy. Int J Sci Res Sci Eng Technol. 2 (2016) 785–789.

[6] Priyadharshini GS, Subramanian R, Murugan N, et al., Influence of Friction Stir Processing Parameters on Surface-Modified 90Cu-10Ni Composites, Mater Manuf Process. 32 (2017) 1416–1427.

[7] Moustafa EB, Mohammed S, Abdel-Wanis S, et al., Taguchi Optimization for AA2024 / Al2O3 Surface Composite Hardness Fabricating by Friction Stir Processing. Int Res J Eng Technol. 11 (2016) 2395–56.

[8] (2018). Vaira Vignesh R, Padmanaban R, Datta M. Influence of FSP on the Microstructure, Microhardness, Intergranular Corrosion Susceptibility and Wear Resistance of AA5083 Alloy, Tribol - Mater Surfaces Interfaces. [Online]. Available: www.doi.org/10.1080/17515831.2018.1483295.

[9] Kumar S, Kumar S. Multi-Response Optimization of Process Parameters for Friction Stir Welding of Joining Dissimilar Al Alloys by Gray Relation Analysis and Taguchi Method. J Brazilian Soc Mech Sci Eng. 37 (2015) 665–674.

[10] (2020). Rathinasuriyan C, Kumar VSS. Optimization of Submerged Friction Stir Welding Parameters of Aluminum Alloy using RSM and GRA. Adv Mater Process Technol. [Online]. Available: www.doi.org/10.1080/2374068X.2020.1793264.

[11] (2020). Dinaharan I, Palanivel R, Murugan N, et al. Application of Artificial Neural Network in Predicting the Wear Rate of Copper Surface Composites Produced Using Friction Stir Processing. Aust J Mech Eng. [Online]. Available: www.doi.org/10.1080/14484846.2020.1769803.

[12] (2018). Martin AR, Moore CP, Finlay WH, et al. Ac ce us. Expert Opin Drug Deliv. [Online]. Available: www.doi.org/10.1080/17425247.2018.1544616.

[13] Rajakumar S, Muralidharan C, Balasubramanian V. Optimization of the Friction-Stir-Welding Process and Tool Parameters to Attain a Maximum Tensile Strength of AA7075-T6 Aluminum Alloy. Proc Inst Mech Eng Part B J Eng Manuf. 224 (2010) 1175–1191.

[14] S. Mishra R, Jain S. Friction Stir Welding (FSW) Process on Aluminum Alloy 6082-T6 using Taguchi Technique. Int J Res Eng Innov. 3 (2019) 301–305.

[15] Yadav.S, Sharma.S, Singh.S, Sharma, PB, Comparison of Mechanical Properties in Single-Pass, Two-Pass and Three-Pass Approach Friction Stir Processing of Aluminium Alloy. 70(1) (2022) 291-298. doi:10.14445/22315381/IJETT-V70I1P234

[16] Miller, J E., Freund, Johnson, R., Probability and Statistics for Engineers [M], 2011: New Delhi: Prentice-Hall. (2011).

[17] Smith WF, Hashemi J. Foundation of Materials Science and Engineering 6th edition: 2019 Published by McGraw-Hill Education, 2 Penn Plaza, New York, NY. 10121.